Molecular theory of Hex*B*-Sm*A*-isotropic transitions in ultrathin liquid crystal films

Jue Shi and Long-pei Shi
Department of Physics, Zhongshan University, Guangzhou, People's Republic of China

D. L. Lin
Department of Physics, State University of New York at Buffalo, Buffalo, New York 14260

(Received 6 May 1999)

A microscopic theory is developed to treat the ultrathin film of liquid crystals of molecules that have no cylindrical symmetry. The Hamiltonian is derived from the basic electrostatic interaction among electrons by considering the dipole-dipole and dipole-quadrupole interactions between nonchiral molecules. It exhibits the in-plane sixfold symmetry. From a unified model with the same interaction constants we are able to explain simultaneously the layer-thinning Sm*A*-*I* transition, the anomalous multiplex heat capacity, the strong singularity in the Hex*B*-Sm*A* transition, and the coexistence of different phases. The theoretical calculations agree quantitatively with recent experimental results for the free-standing 54COOBC films.
[S1063-651X(99)18410-1]

PACS number(s): 64.70.Md, 64.60.Cn, 61.30.−v

1. INTRODUCTION

During the past 40 years the characteristics and behavior of liquid crystals (LC) have been an interesting topic to many researchers. Compared to the increasing number of unusual phenomena observed in LC, theoretical development is still limited and cannot account for some novel LC anomaly. One of the significant theoretical works was done by Maier and Saupe [1], who introduced the orientational order parameter to described the alignment of the molecules parallel to a preferred axis in the nematic phase. Goosens [2] extend this theory to calculate the dispersion interaction energy between two optically active anisotropic molecules with chirality, and successfully explained the helical structure of the cholesteric phase, a special case of the nematic phase. Later, Mcmillan [3] introduced a new order parameter, the amplitude of a density wave in the direction of the nematic preferred axis for the Sm*A* phase. Though there exist some phenomenological theories for Hex*B* or Herringbone phase [4,5] to explain the positional and orientational order, the physical features remain obscure. Hence, it is necessary to develop a microscopic model for Hex*B* phase, which possesses the sixfold symmetry.

In a previous paper [6], we proposed a unified molecular model for noncylindrically symmetric liquid crystal molecules in freely suspended films to explain the unusual phenomenon observed on 54COOBC during the Hex*B*-Sm*A*-*I* transitions. The theoretical results of a layer-thinning effect in the Sm*A*-*I* transition are in good agreement with the experimental data [7,8]. However, the relatively flat temperature dependence of the heat capacity did not reconcile well with sharp peaks observed in experiments on the Hex*B*-Sm*A* transition. Therefore in this paper, aside from a more elaborate discussion of the unified molecular model, we focus on the study of the coupling constant dependence of the heat-capacity anomaly.

In general, the smectic phase exists of the layer positional order and the molecular directional order, which are described by the order parameters

$$\sigma=\left\langle \cos\left(\frac{2\pi z}{d}\right)\left(\frac{3}{2}\cos^2\theta-\frac{1}{2}\right)\right\rangle \quad \text{and} \quad \Theta=\left\langle \frac{3}{2}\cos^2\theta-\frac{1}{2}\right\rangle,$$

respectively. For 54COOBC, the Sm*A* phase changes directly into the isotropic phase (without the intermediate nematic phase). The layer-positional order parameter σ depends on the temperature in a completely similar fashion as the directional order Θ. Thus, the layer-positional order and directional order can exist simultaneously [$\Theta(T)=0$, $\sigma(T)=0$ and $\Theta(T)\neq 0$, $\sigma(T)\neq 0$]. In this case we simply ignore the layer-positional order, and apply only the directional order to describe the smectic phase. Otherwise, the Hex*B* phase is characterized by the existence of molecular hexatic-positional order, described by the order parameter $\Phi=\langle\cos 3\varphi\rangle$ [6], which is different from the assumption of, Nelson and Co-workers [4]. Since there is no net charge or permanent dipole, the interaction between the molecules is certainly the dispersion interaction and the interaction energy can be obtained by perturbation. In our theory the interaction energy of smectic order (the long-axis tilt angle θ), which accounts for the Sm*A*-*I* transitional phenomenon, is deduced from the second-order perturbation of a dipole-dipole interaction, while the interaction energy of hexatic order (the long-axis rotation angle φ), which accounts for the Hex*B*-Sm*A* transition, is deduced from the second-order perturbation of a dipole-quadrupole interaction.

In addition, due to the reduced symmetry of the surface layer, there exists a surface component of the interaction energy, which must be taken into account. For ultrathin films, the surface potential is of significant importance [6]. By carefully considering the experimental results that ultrathin 54COOBC films have higher transition temperatures than the bulk, we assume that 54COOBC possesses a strong surface potential and the order parameter of the surface exceeds those of the interior layers.

II. THEORETICAL MODEL

A series of experiments [9–12] have confirmed that the Hex*B* phase of 54COOBC possesses sixfold diffraction and

has positional order. Therefore, it is reasonable to take a molecular-layer model and assume that the molecular density distribution possesses a hexagonal close-packed structure as illustrated in Fig. 1(a). The molecule (0,0,0) in this model has twelve nearest neighbors located at $(a,0,0)$, $(-a,0,0)$,

$$\left(-\frac{1}{2}a,\frac{\sqrt{3}}{2}a,0\right),\left(\frac{1}{2}a,-\frac{\sqrt{3}}{2}a,0\right),$$

$$\left(-\frac{1}{2}a,-\frac{\sqrt{3}}{2}a,0\right),\left(\frac{1}{2}a,\frac{\sqrt{3}}{2}a,0\right) \text{ in the same layer,}$$

$$\left(0,\frac{1}{\sqrt{3}}a,c\right),\left(-\frac{1}{2}a,-\frac{1}{2\sqrt{3}}a,c\right),$$

$$\left(\frac{1}{2}a,-\frac{1}{2\sqrt{3}}a,c\right) \text{ in the upper layer, and}$$

$$\left(0,\frac{1}{\sqrt{3}}a,-c\right),\left(-\frac{1}{2}a,-\frac{1}{2\sqrt{3}}a,-c\right),$$

$$\left(\frac{1}{2}a,-\frac{1}{2\sqrt{3}}a,-c\right) \text{ in the lower layer,}$$

where a is the distance between molecule i and its nearest neighbors in the same layer, and c is the interlayer distance. Moreover, the molecule without chirality is supposed to possess a long-axis ζ and short-axes ξ and η. It has the reflection symmetry with respect to the ζ ξ plane, but has no such symmetry in η. In other words, the constituent molecules do not have the cylindrical symmetry because the cross section of the molecule is assumed to be triangular rather than circular.

By expanding the electrostatic interaction

$$\hat{H}_{ij}=\sum_{k,l}\frac{e_{ik}e_{jl}}{|\vec{R}_{jl}-\vec{R}_{ik}|}$$

in the Taylor series, we have [2]

$$\hat{H}_{ij}=a_{ij}R_{ij}^{-3}+(b_{ij}^{pq}+b_{ij}^{qp})R_{ij}^{-4}+\cdots \tag{1}$$

with

$$a_{ij}=\vec{p}_i\cdot\vec{p}_j-3\vec{p}_i\cdot\vec{u}_{ij}\vec{p}_j\cdot\vec{u}_{ij}, \tag{2a}$$

$$b_{ij}^{pq}=-\tfrac{3}{2}\{q_j\vec{p}_i\cdot\vec{u}_{ij}+2\vec{p}_i\cdot\vec{\vec{Q}}_j\cdot\vec{u}_{ij}-5\vec{p}_i\cdot\vec{u}_{ij}(\vec{u}_{ij}\cdot\vec{\vec{Q}}_j\cdot\vec{u})\}, \tag{2b}$$

$$b_{ij}^{qp}=\tfrac{3}{2}\{q_i\vec{p}_j\cdot\vec{u}_{ij}+2\vec{p}_j\cdot\vec{\vec{Q}}_i\cdot\vec{u}_{ij}-5\vec{p}_j\cdot\vec{u}_{ij}(\vec{u}_{ij}\cdot\vec{\vec{Q}}_i\cdot\vec{u}_{ij})\}, \tag{2c}$$

where we have defined the electric dipole $\vec{p}_i=\Sigma_k e_{ik}\vec{\rho}_{ik}$ and the electric quadrupole $\vec{\vec{Q}}_j=\Sigma_l e_{jl}\vec{\rho}_{jl}\vec{\rho}_{jl}$ with

$$q_j=\Sigma_l e_{jl}\vec{\rho}_{jl}\cdot\vec{\rho}_{jl}.$$

Other notation includes the intermolecular distance $R_{ij}=|\vec{R}_j-\vec{R}_i|$ and the unit vector $\vec{u}_{ij}=(\vec{R}_j-\vec{R}_i)/R_{ij}$. It is assumed that the molecules are neutral and there is no permanent dipoles, so that $\Sigma_k e_{ik}=0$ and $\Sigma_k\langle 0|\vec{\rho}_{ik}|0\rangle=0$.

To the second-order perturbation, the interaction energy H_{ij} takes the form

$$H_{ij}=H_{ij}^a+H_{ij}^b+\cdots, \tag{3}$$

where

$$H_{ij}^a=\frac{1}{R_{ij}^6}\sum_\mu\frac{\langle 0|a_{ij}|\mu\rangle\langle\mu|a_{ij}|0\rangle}{E_0-E_\mu}, \tag{4a}$$

$$H_{ij}^b=\frac{1}{R_{ij}^8}\sum_\mu\frac{\langle 0|b_{ij}^{pq}|\mu\rangle\langle\mu|b_{ij}^{qp}|0\rangle+\text{c.c.}}{E_o-E_\mu}, \tag{4b}$$

and for molecules without chirality [2]

$$H_{ij}^{ab}=\frac{1}{R_{ij}^7}\sum_\mu\frac{\langle 0|a_{ij}|\mu\rangle\langle\mu|b_{ij}^{pq}+b_{ij}^{qp}|0\rangle}{E_0-E_\mu}=0. \tag{4c}$$

It is convenient to define the position of the point charges with respect to the position $\vec{R}_{ik}$ in a coordinate system ξ, η, ζ, which is fixed to the molecule. Then $\vec{R}_{ik}=\vec{R}_i+\vec{\rho}_{ik}(x_{ik}y_{ik}z_{ik})$, which is defined in the fixed macroscopic coordinate system, and can be expressed by means of the Euler transformation with Euler angles φ_i, θ_i, ψ_i as $\vec{R}_{ik}=\vec{R}_i+\vec{\rho}_{ik}(\xi_{ik}\eta_{ik}\zeta_{ik})$, in which $\vec{\rho}_{ik}(\xi_{ik}\eta_{ik}\zeta_{ik})$ is defined in the molecular coordinate system. According to the Euler transformation,

$$\begin{aligned}x_{ik}&=\cos\theta_i\cos\varphi_i\xi_{ik}-\sin\varphi_i\eta_{ik}+\sin\theta_i\cos\varphi_i\zeta_{ik},\\ y_{ik}&=\cos\theta_i\sin\varphi_i\xi_{ik}+\cos\varphi_i\eta_{ik}+\sin\theta_i\sin\varphi_i\zeta_{ik},\\ z_{ik}&=-\sin\theta_i\xi_{ik}+\cos\theta_i\zeta_{ik},\end{aligned} \tag{5}$$

when $\psi=0$ has been assumed. In this coordinate system, the interaction energy of molecule i with its six nearest neighbor molecules j in the same layer ($R_{ij}=a$) are the same as

$$H_{ij}^a=-D_{ij}P_iP_j, \tag{6a}$$

$$\begin{aligned}\tfrac{4}{9}H_{ij}^b=&-12[C_{ij}^{(1)}P_iP_j+(C_{ij}^{(2)}P_i+C_{ji}^{(2)}P_j)+C_{ij}^{(3)}]F_iF_j\\&+13[C_{ij}^{(1)}P_iP_j+(C_{ij}^{(2)}P_i+C_{ji}^{(2)}P_j)+C_{ij}^{(3)}]F_{si}F_{sj}.\end{aligned} \tag{6b}$$

Let

$$B_{ij}=27C_{ij}^{(1)},\quad C_{ij}=27C_{ij}^{(2)},\quad \text{and } Q_{ij}=27C_{ij}^{(3)}.$$

The interaction energy of molecule i with its six nearest neighbor molecules j in the adjacent layer ($R_{ij}\approx c$) are the same as

$$H_{ij}^a=-2D_{ij}P_iP_j \tag{7a}$$

$$\frac{4}{9}H_{ij}^{b}=\frac{8}{\left(1+\frac{3c^2}{a^2}\right)}\{[C_{ij}^{(1)}P_iP_j+(C_{ij}^{(2)}P_i+C_{ji}^{(2)}P_j)+C_{ij}^{(3)}]\times F_iF_j+[C_{ij}^{(1)}P_iP_j+(C_{ij}^{(2)}P_{2i}+C_{ji}^{(2)}P_{2j})+C_{ij}^{(3)}]F_{si}F_{sj}\},\tag{7b}$$

where we have assumed that $c\gg a$.

Now let

$$B_{ij}=-\frac{18}{\left(1+\frac{3c^2}{a^2}\right)}C_{ij}^{(1)},\quad C_{ij}=-\frac{18}{\left(1+\frac{3c^2}{a^2}\right)}C_{ij}^{(2)},$$

$$Q_{ij}=-\frac{18}{\left(1+\frac{3c^2}{a^2}\right)}C_{ij}^{(3)},$$

where

$$D_{ij}=\frac{1}{R_{ij}^6}\sum_{\mu}\frac{1}{E_\mu-E_0}\{[\langle 0|p_{\zeta i}|\mu\rangle\langle\mu|p_{\zeta i}|0\rangle-\langle 0|p_{\xi i}|\mu\rangle\times\langle\mu|p_{\xi i}|0\rangle][\langle 0|p_{\zeta j}|\mu\rangle\langle\mu|p_{\zeta j}|0\rangle-\langle 0|p_{\xi j}|\mu\rangle\times\langle\mu|p_{\xi j}|0\rangle]\},\tag{8}$$

$$C_{ij}^{(1)}=\frac{1}{R_{ij}^8}\sum_{\mu}\frac{1}{E_\mu-E_0}(C_{1i}C_{1j}^{*}+\text{c.c.}),\tag{9a}$$

$$C_{ij}^{(2)}=\frac{1}{R_{ij}^8}\sum_{\mu}\frac{1}{E_\mu-E_0}(C_{1i}C_{2j}^{*}+\text{c.c.}),\tag{9b}$$

$$C_{ji}^{(2)}=\frac{1}{R_{ij}^8}\sum_{\mu}\frac{1}{E_\mu-E_0}(C_{2i}C_{1j}^{*}+\text{c.c.}),\tag{9c}$$

$$C_{ij}^{(3)}=\frac{1}{R_{ij}^8}\sum_{\mu}\frac{1}{E_\mu-E_0}(C_{2i}C_{2j}^{*}+\text{c.c.}),\tag{9d}$$

$$12C_{1i}=4\langle 0|p_{\xi i}|\mu\rangle\langle\mu|q_{\xi\eta i}|0\rangle+2\langle 0|p_{\eta i}|\mu\rangle\langle\mu|q_{\xi\xi i}|0\rangle-4\langle 0|p_{\zeta i}|\mu\rangle\langle\mu|q_{\zeta\eta i}|0\rangle-2\langle 0|p_{\eta i}|\mu\rangle\langle\mu|q_{\zeta\zeta i}|0\rangle,\tag{10a}$$

$$12C_{2i}=2\langle 0|p_{\xi i}|\mu\rangle\langle\mu|q_{\xi\eta i}|0\rangle+4\langle 0|p_{\zeta i}|\mu\rangle\langle\mu|q_{\zeta\eta i}|0\rangle+\langle 0|p_{\eta i}|\mu\rangle\langle\mu|q_{\xi\xi i}|0\rangle+2\langle 0|p_{\eta i}|\mu\rangle\langle\mu|q_{\zeta\zeta i}|0\rangle-3\langle 0|p_{\eta i}|\mu\rangle\langle\mu|q_{\eta\eta i}|0\rangle,\tag{10b}$$

$$P_i=\frac{3\cos^2\theta_i-1}{2},\quad F_i=\cos 3\varphi_i,\quad F_{si}=\sin 3\varphi_i.$$

Note that for molecule i, $p_{\alpha i}=\Sigma_k e_{ik}\alpha_{ik}$ denotes the electric dipole moment component and $q_{\alpha\beta i}=\Sigma_k e_{ik}\alpha_{ik}\beta_{ik}$ the electric quadrupole moment components with $\alpha,\beta=\xi,\eta,\zeta$.

The ground state of the surface molecule satisfies the equation $|s\rangle=c_0|0\rangle+c_1|1\rangle$, where $|0\rangle$ is the ground state of molecules in the interior layers. The reduced symmetry of the surface requires that an additional surface energy

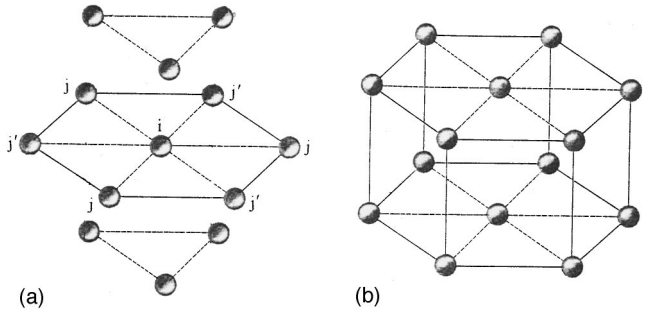

FIG. 1. The assumed molecular arrangement.

$$H_i^{s}=-\frac{1}{2}\sum_{i,j}S_{ij}^{p}P_iP_j-\frac{1}{2}\sum_{i,j}S_{ij}^{q}F_iF_j,\tag{11}$$

where S_{ij}^{p} and S_{ij}^{q} can be derived from D_{ij} and Q_{ij}, respectively, by replacing $|0\rangle$ by $|s\rangle$. Combining the above results, the complete Hamiltonian is obtained as [6]

$$H=-\frac{1}{2}\sum_{i,j}D_{ij}P_iP_j-\frac{1}{2}\sum_{i,j}Q_{ij}F_iF_j-\frac{1}{2}\sum_{i,j}B_{ij}P_iP_jF_iF_j-\sum_{i,j}C_{ij}P_jF_iF_j-\frac{1}{2}\sum_{i,j}S_{ij}^{p}P_iP_j-\frac{1}{2}\sum_{i,j}S_{ij}^{q}F_iF_j,\tag{12}$$

where $P_i=(3\cos^2\theta_i-1)/2$, $F_i=\cos 3\varphi_i$.

Assuming the interaction between nearest molecules in our molecular model from Eqs. (6a)–(10b) we have proved that for the interlayer interaction $D_{ij}=2D'>0$, $Q_{ij}=Q'<0$, $B_{ij}=B'<0$, and $C_{ij}=C'\approx 0$, while for the intralayer interaction $D_{ij}=D>0$, $Q_{ij}=Q>0$, $B_{ij}=B>0$, and $C_{ij}=C$. Furthermore, $S_{ij}^{p}=S^{p}>0$ and $S_{ij}^{q}=S^{q}>0$ for the existence of a stable surface. In addition, it can also be shown in the approximation $c\gg a$ that $D>D'$, $Q\gg|Q'|$, and $B\gg|B'|$. Hence, only one term with the coefficient D_{ij} is important in the calculation of the interlayer interaction, and all other terms of the interlayer interaction are negligible. Since the statistical average value of $F_{si}=\sin 3\varphi_i$ is approximately zero, all terms involving $F_{si}F_{sj}$ in the Hamiltonian have been neglected to a reasonably good approximation.

Applying the molecular field approximation to the Hamiltonian obtained above, we perform a self-consistent calculation numerically for the temperature dependence of the order parameters for the N-layer film. Since we are studying the freely suspended N-layer film, the nth molecular layer in the film is equivalent to the $(N+1\text{-}n)$th layer. And molecules in the same molecular layer are all equivalent because of the translational symmetry. Then

$$\Theta_n(T)=\langle P_n\rangle\ \text{ and }\ \Phi_n(T)=\langle F_n\rangle\quad[n=1,2,3,\ldots,N/2,\ \text{or}\ (N+1)/2],\tag{13}$$

where

$$\langle A_n\rangle=\frac{\int_0^{\pi}\int_0^{2\pi}A_n e^{-V_n/k_BT}\sin\theta_n d\theta_n d\varphi_n}{\int_0^{\pi}\int_0^{2\pi}e^{-V_n/k_BT}\sin\theta_n d\theta_n d\varphi_n},$$

and $A_n=P_n$, F_n, and V_n. From Eq. (12) we have (a) for the bulk,

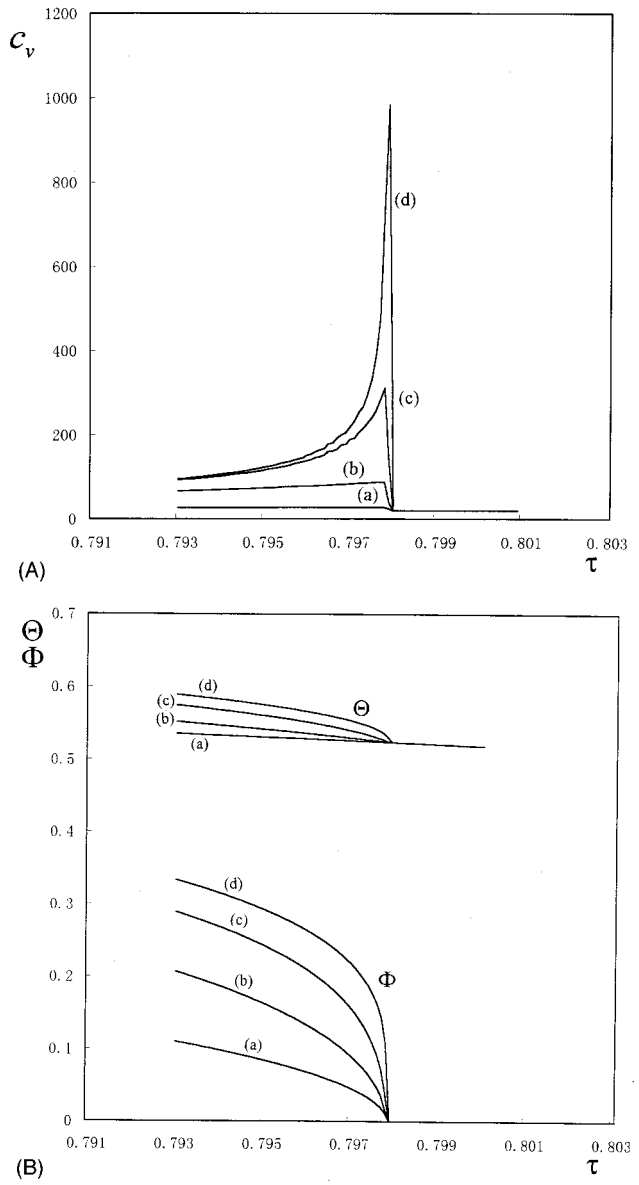

FIG. 2. (A) The reduced heat capacity c_v of each layer of bulk versus reduced temperature τ with the same transition temperature of bulk ($\tau_{\mathrm{HS}}=0.7979$, $\tau_{\mathrm{Sl}}=0.8357$). (B) Θ and Φ of bulk versus reduced temperature τ ($\tau_{\mathrm{HS}}=0.7979$, $\tau_{\mathrm{Sl}}=0.8357$) with $D=0.035\,36$ eV and $D'/D=0.125$; (a) $B/D=0$, $Q/D=0.5319$; (b) $B/D=0.298$, $Q/D=0.45$; (c) $B/D=0.4$; $Q/D=0.422$; and (d) $B/D=0.44$, $Q/D=0.411$.

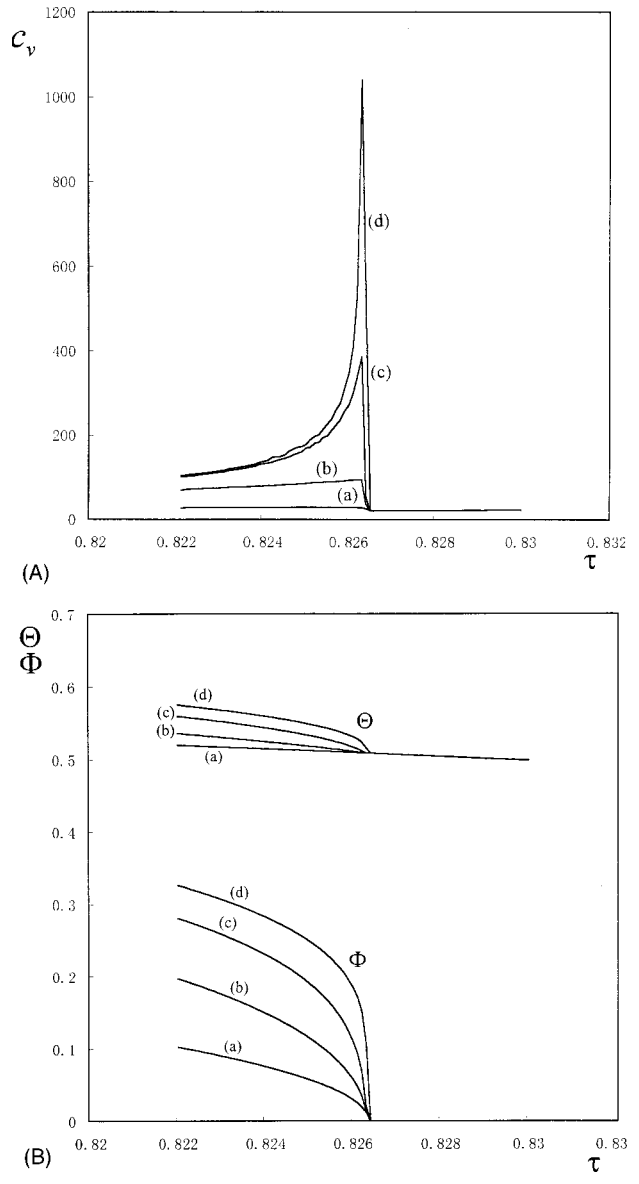

FIG. 3. (A) The reduced heat capacity c_v of a two-layer film versus reduced temperature τ with the same transition temperature of a two-layer film ($\tau_{\mathrm{HS}}=0.8264$, $\tau_{\mathrm{Sl}}=0.8591$). (B) Θ and Φ of a two-layer film versus reduced temperature τ ($\tau_{\mathrm{HS}}=0.8264$, $\tau_{\mathrm{Sl}}=0.8591$), with $D=0.035\,36$ eV, $D'/D=0.125$, and $S^p/D=0.16$. (a) $B/D=0$, $Q/D=0.5319$, and $S^q/D=0.019$; (b) $B/D=0.298$, $Q/D=0.45$, and $S^q/D=0.0238$; (c) $B/D=0.4$, $Q/D=0.422$, and $S^q/D=0.0254$; and (d) $B/D=0.44$, $Q/D=0.411$, and $S^q/D=0.026$.

$$\Theta=\Theta_n=\langle P_n\rangle,\quad \Phi=\Phi_n=\langle F_n\rangle,$$

$$V=V_n=-3D\Theta_nP_n-6D'\Theta_nP_n-3B\Theta_n\Phi_nP_nF_n-3Q\Phi_nF_n,$$

(b) for the two-layer film,

$$\Theta_1=\Theta_2=\langle P_1\rangle,\quad \Phi_1=\Phi_2=\langle F_1\rangle,$$

$$V_1=V_2=-3D\Theta_1P_1-3D'\Theta_2P_1-3B\Theta_1\Phi_1P_1F_1-3Q\Phi_1F_1-3S^p\Theta_1P_1-3S^q\Phi_1F_1,$$

and (c) for the N-layer film ($N\geqslant 3$),

$$\Theta_n=\langle P_n\rangle=\langle P_{N+1-n}\rangle,\quad \Phi_n=\langle F_n\rangle=\langle F_{N+1-n}\rangle.$$

The single-molecule potential of the surface layer is

$$V_1=-3D\Theta_1P_1-3D'\Theta_2P_1-3B\Theta_1\Phi_1P_1F_1-3Q\Phi_1F_1-3S^p\Theta_1P_1-3S^q\Phi_1F_1,$$

while the single-molecule potential of the nth interior layer is

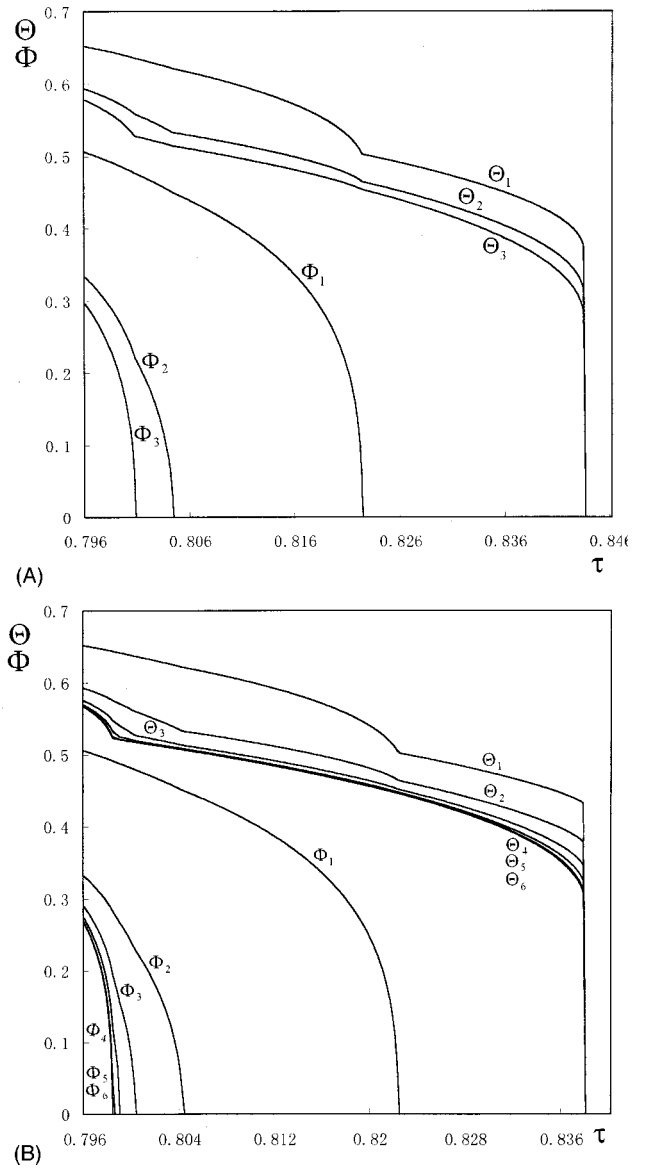

FIG. 4. (A) Θ_n and Φ_n of a 6-layer film versus reduced temperature τ with $D=0.035\,36$ eV, $D'/D=0.125$, $S^p/D=0.16$, $B/D=0.44$, $Q/D=0.411$, and $S^q/D=0.026$. (B) Θ_n and of an 11-layer film versus reduced temperature τ.

$$V_n=V_{N+1-n}=-3D\Theta_nP_n-3D'(\Theta_{n+1}+\Theta_{n-1})P_n$$

$$-3B\Theta_n\Phi_nP_nF_n-3Q\Phi_nF_n$$

$$[n=2,\ldots,N/2,\ \text{or}\ (N+1)/2].$$

It is clear that there are altogether N (or $N+1$) coupled equation (13) for Θ_n and Φ_n, when N is even (or odd). After determination of $\Theta_n(T)$ and $\Phi_n(T)$ at temperature T, we can simultaneously calculate the internal energy per square centimeter $U(T)=\rho\Sigma_{n=1}^{N}\langle V_n\rangle$, in which density ρ is the number of molecules per sq cm of each layer, and the specific heat $C_v=(\partial U/\partial T)_v$, as well as the transition temperature for comparison with the experimental data.

The choice of the positional order parameter $\Phi=\langle\cos 3\varphi\rangle$ is based on a Hamiltonian with sixfold symmetry. As revealed by Eq. (4), the interaction energy H_{ij} possesses space inversion symmetry, which means that the interaction between the molecule i and the neighboring molecule j remains unchanged under space inversion. An example is shown in Fig. 1(a) when j becomes j'. Therefore, the order parameter $\Phi=\langle\cos 3\varphi\rangle$ with threefold symmetry has already indicated the order between the molecule i and its three neighbors j as well as j'. Consequently, the molecular density distribution with threefold symmetry and inversion sym-

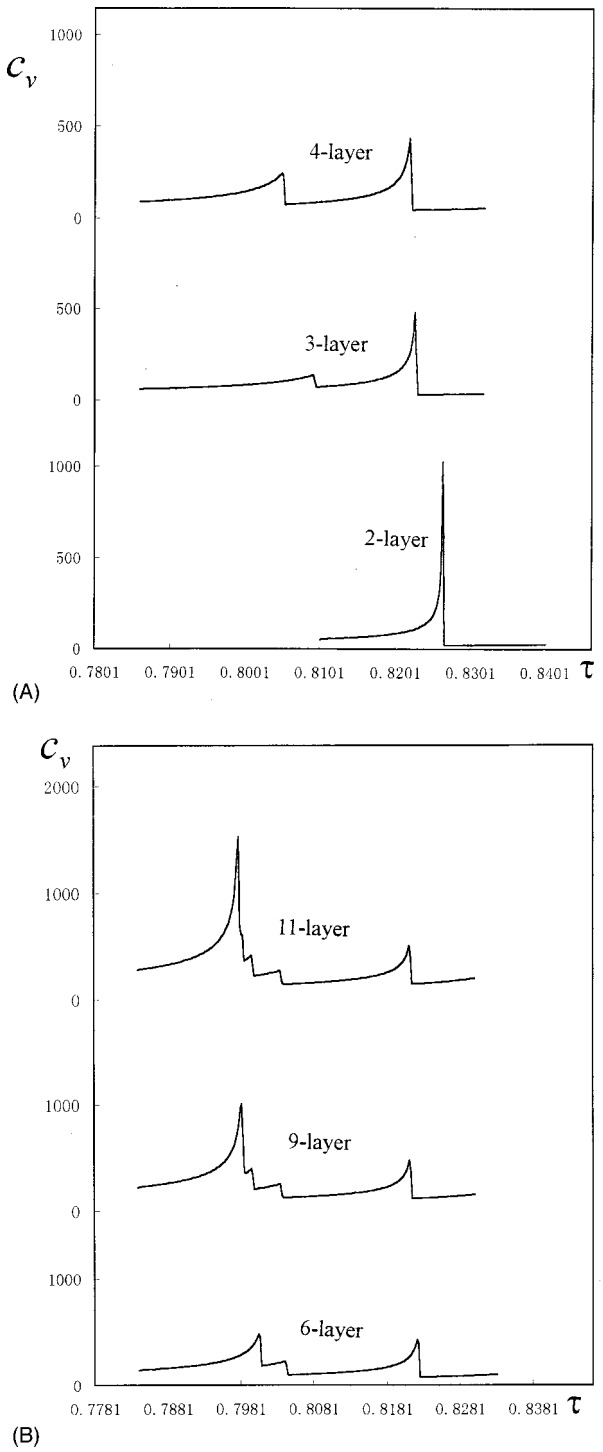

FIG. 5. (A) The reduced heat capacity c_v of two, three- and four-layer film versus the reduced temperature τ. (B) The reduced heat capacity c_v of 6, 9, and 11-layer film versus the reduced temperature τ.

TABLE I. Peak temperatures $\tau_{n,\mathrm{HP}}$ [$T_{n,\mathrm{HP}}=(D/k_B)\tau_{n,\mathrm{HB}}$] of the nth layer in an N-layer film. The heat-capacity peaks of 5th and 6th layer are indistinguishable.

N	12	11	10	9	8	7	6	5	4	3	2	∞ (Bulk)
$\tau_{1,\mathrm{HP}}$	0.8223	0.8223	0.8223	0.8223	0.8223	0.8223	0.8223	0.8224	0.8226	0.8234	0.8263	0.7978
$T_{1,\mathrm{HP}}$ (°C)	64.50	64.50	64.50	64.50	64.50	64.50	64.50	64.54	64.62	64.95	66.14	54.44
$\tau_{2,\mathrm{HP}}$	0.8042	0.8042	0.8042	0.8042	0.8042	0.8042	0.8043	0.8045	0.8055	0.8098		
$T_{2,\mathrm{HP}}$ (°C)	57.07	57.07	57.07	57.07	57.07	57.07	57.11	57.19	57.60	59.37		
$\tau_{3,\mathrm{HP}}$	0.8001	0.8001	0.8001	0.8001	0.8002	0.8004	0.8007	0.8021				
$T_{3,\mathrm{HP}}$ (°C)	55.39	55.39	55.39	55.39	55.43	55.51	55.63	56.21				
$\tau_{4,\mathrm{HP}}$	0.7989	0.7989	0.7989	0.7990	0.7991	0.7996						
$T_{4,\mathrm{HP}}$ (°C)	54.90	54.90	54.90	54.94	54.98	55.18						
$T_{5,\mathrm{HP}}$	0.7982	0.7983	0.7985	0.7987								
$T_{5,\mathrm{HP}}$ (°C)	54.61	54.65	54.73	54.81								

metry exhibits sixfold symmetry diffraction as a whole.

All the constants can be derived theoretically when the molecular states are known. We determine these coupling constants in the following from the experimental data for the bulk and two-layer film of 54COOBC [7,8]. For convenience, we define the reduced temperature $\tau=(k_B/D)T$, the reduced internal energy $u=U/\rho D$, and the reduce heat-capacity $c_v=\partial u/\partial\tau=C_v/\rho k_B$ instead of temperature T, internal energy U, and heat capacity C_v, respectively, in the numerical calculation. For example, if $\rho\approx 5\times 10^{13}\,\mathrm{cm}^2$, we have $c_v\approx 1.45\times 10^3 C_v(\mathrm{cm}^2\,\mathrm{K}/\mu\mathrm{J})$ with $k_B=1.38\times 10^{-17}(\mu\mathrm{J/K})$.

We first determine D and D' from the bulk SmA-I transition temperature 70 °C [7,8]. For instance, we adjust $D'/D=0.125$; then, from the calculation for $\Theta_n(\tau)$ above the Hex$B$-SmA transition temperature, the bulk SmA-I transition temperature of $\tau_{\mathrm{SI}}=0.8357$ can be found independent of constants Q, B, and $S^p=S^q=0$. Since $T_{\mathrm{SI}}=(D/k_B)\tau_{\mathrm{SI}}$ corresponds to 70 °C and $k_B=8.6164\times 10^{-5}$ eV/K, we find $D=0.035\,36$ eV. In this case the relation between temperature T and the reduced temperature τ is $T=(410.43\tau)$ K $=(410.43\tau-273)$ °C. On the other hand, the value of D'/D cannot be chosen arbitrarily as it may change the detail of the transitional behavior. According to experiments [7,8], our calculation shows that $D'/D\sim 0.1$.

Second, Q as well as B are determined by τ_{HP}, the temperature at which the heat capacity for bulk Hex$B$-SmA transition peaks. Note that $\tau_{\mathrm{HP}}=0.7975$ corresponds to $T_{\mathrm{HP}}=54.3$ °C [8]. The B dependence of the transition order and the shape of the heat-capacity peak is depicted in Fig. 2. It is clearly seen that a larger B ($B/D>0.4$) results in a sharper peak, and that the corresponding transition changes from a second order to a weak first order. Hence, the sharp peaks of the experimental heat capacity in Ref. [8] implies that $B/D=0.44$ and then $Q/D=0.411$ when $D'/D=0.125$ and $\tau_{\mathrm{HP}}=0.7975$. Though both B and C are the coupling constants between long-axis directional order and hexatic-positional order, which account for the detailed shape of the heat-capacity peaks in the Hex$B$-SmA transition, the part of $P_iP_jF_iF_j$ is actually responsible for the sharp heat-capacity peak, which is consistent with the experimental observation, while the part of $P_jF_iF_j$ gives a rather flat peak. Therefore, the contribution of $P_jF_iF_j$ should be smaller than the contribution of $P_iP_jF_iF_j$. Moreover, the sign of C cannot be fixed in our model. For this reason, we simply neglect the part of $P_jF_iF_j$ in the calculation. In other words, we let $C=C'=0$.

Finally, the surface constant S^p is determined by the SmA-I transition temperature $\tau_{\mathrm{SI}}=0.8594$ or $T_{\mathrm{SI}}=79.72$ °C of the two-layer film [7,8]. The other surface constant S^q is determined by the heat-capacity peak temperature $\tau_{\mathrm{HP}}=0.8267$ or $T_{\mathrm{HP}}=66.3$ °C observed in the Hex$B$-SmA transition for a two-layer film [8]. Thus, we have $S^p/D=0.16$ and $S^q/D=0.026$ when D, D', Q, and B are chosen as above. Employing the coupling constants thus determined, we calculate the order parameter and the temperature-dependent heat capacity. It is found, as is indicated in the experiment [8], that the Hex$B$-SmA transition of a two-layer film is weak first order as shown in Fig. 3(b). Since S^p is sufficiently large to provide strong surface potential, the effect of surface enhancement outweighs the interlayer interactions. This explains why the internal energy of interior layers becomes lower than the bulk, and eventually renders the layer-thinning phenomenon, and the phase transition in ultrathin films takes place above the bulk transition temperature.

As indicated above, there may be more than one set of coupling constants that yield the consistent results with the experimental data for 54COOBC films [7,8]. In the present paper, we pick the following set for our computation.

D/eV	$\frac{D}{D}$	$\frac{Q}{D}$	$\frac{B}{D}$	$\frac{S^p}{D}$	$\frac{S^q}{D}$
0.035 36	0.125	0.411	0.44	0.16	0.026

III. THEORETICAL RESULTS

In Fig. 4, the order parameters Θ_n and Φ_n for (a) a 6-layer and (b) 11-layer films all vanish above the bulk SmA-I and Hex$B$-SmA transition temperatures, due to the surface-enhanced order. Due to the interlayer coupling of smectic order, Θ_n for all n disappears simultaneously, while Φ_n for different n vanishes at different temperatures due to the lack of direct interlayer interaction in the hexatic order.

The surface layer, on the other hand, must experience the Hex*B*-Sm*A* transition at the highest temperature due to the enhancement of the surface potential. The size of Φ_n follow the order $\Phi_1(T)>\Phi_2(T)>\Phi_3(T)>\Phi_4(T)>\Phi_5(T)>\Phi_6(T)$, the interior layers change into a Sm*A* phase while the outermost layer remains in a Hex*B* phase. Therefore, the coexistence of Sm*A* and Hex*B* phases is understood theoretically.

In the case that the coupling between directional order (θ) and positional as well as orientational order (φ) is weak enough such as those shown in Figs. 2 and 3 for $B<0.3$, the Hex*B*-Sm*A* transition is of second order in nature. This corresponds to the KT transition [15] because the order parameter Φ_n vanishes continuously and the temperature-dependent heat capacity has the characteristic hump. On the other hand, the Sm*A*-*I* transition is of strong first order in nature as the order parameter Θ_n drops sharply to zero and the heat capacity peak diverges. In the case that the coupling between θ and φ is strong enough or B is large enough, the Hex*B*-Sm*A* transition would becomes weak first order. An example for $B>0.4$ is shown in Figs. 2 and 3. Our calculation seems to confirm the experimental findings of 54COOBC that the Hex*B*-Sm*A* transition is first order rather than of second order.

The Hex*B*-Sm*A* transition in free-standing liquid crystal films behaves quite differently. As is shown in Fig. 5, the heat capacity exhibits multiplex peaks implying the layer-by-layer melting phenomenon. The transition temperature for films of 2–11 layers calculated for the same set of parameters are listed in Table I, and they differ from the corresponding experimental values by about 1 °C. The calculated heat capacity peaks of 3–11-layer films are compared with the data available in Ref. [8]. It is found that quantitative agreement is achieved by assuming $C_p \approx C_v$ and $\rho \approx 5\times10^{13}\,\mathrm{cm}^2$, which corresponds to $a \approx 15\,\text{Å}$. Only the 2-layer film has a higher peak than the experiment.

The above results demonstrate that thinner films possess higher transitions and the Sm*A*-*I* transition occurs through a series of a layer-thinning process. In other words, the free-standing liquid crystal films thin in a stepwise manner as the temperature increases. The situation is illustrated in Fig. 6. In Table II the transition temperatures calculated from the same set of coupling constants are compared with the experimental layer-thinning transition data of Ref. [7]. It is seen that the agreement is generally good and the discrepancy is within 1 °C.

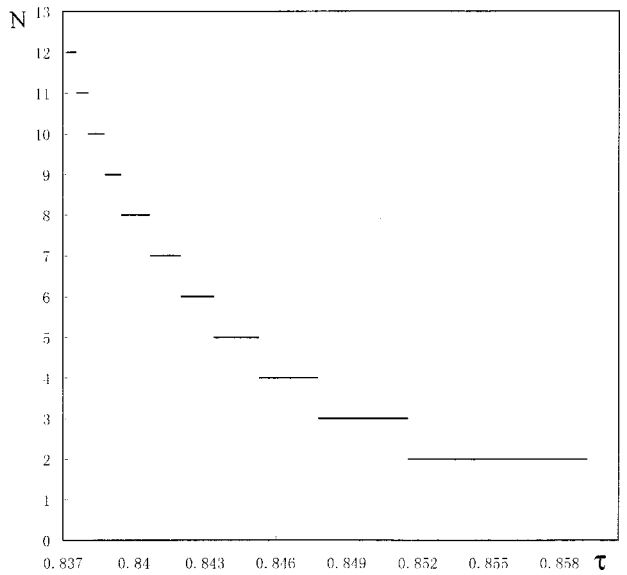

FIG. 6. The thickness of a stable film (N) versus reduced temperature τ.

IV. CONCLUSION AND DISCUSSION

We have studied the dependence of the multiplex heat-capacity anomaly on coupling constants in the Hex*B*-Sm*A* transition and the coexistence of a different phase in freely suspended film of liquid crystal. In our theory we introduce two order parameters, the directional order $P(\theta)$ of the molecular long axis and the positional order $F(\varphi)$ of the molecules, to describe, respectively, the smectic and hexatic phase of liquid crystals. From theoretical calculations, we have investigated (i) the lack of direct interlayer interaction component for hexatic order or $Q' \leqslant 0$, (ii) the enhancement of the surface potential or large enough positive S^p and S^q, (iii) the existence of a direct interlayer interaction component for smectic order or $D'>0$, and (iv) the existence of the coupling between the intralayer hexatic and smectic order or large enough B. By applying our theory to 54COOBC liquid crystal, the calculated results are quantitatively consistent with the experimental observations. We also show by the vanishing hexactic positional order that the Hex*B*-Sm*A* transition is second order or weak first order and the latter applies to 54COOBC ultrathin films as is already evidenced by observations [13].

The different behavior between individual molecular layers in the Hex*B*-Sm*A* transition is a result of the strong surface-enhancing effect. The surface potential with constant S^p originally strengthens the smectic order of different interior layers (determined by D'). It enhances the hexatic order of different interior layers through the hexatic-smectic coupling effect (determined by B), and thus causes the distinction among molecular layers in the film. Consequently, the phase transition of molecular layers takes place at different temperatures and displays heat-capacity peaks of different magnitudes, which renders the appearance of the multiple heat-capacity anomaly. Though the other surface potential S^q also contributes directly to the surface enhancement, its con-

TABLE II. Sm*A*-*I* transition temperatures $\tau_{SI}[T_{SI}=(D/k_B)\tau_{SI}]$ of an N-layer film.

N	12	11	10	9	8	7	6	5	4	3	2	∞ (Bulk)
τ_{SI}	0.8375	0.8380	0.8387	0.8395	0.8407	0.8419	0.8433	0.8452	0.8477	0.8515	0.8591	0.8357
$T_{SI}(°C)$	70.74	70.94	71.23	71.56	72.05	72.54	73.12	73.90	74.92	76.48	79.60	70.00

tribution is rather small compared with S^p and is of less significance.

From the above discussion, we emphasize that when the constant B is positive and larger enough, we predict a strong singularity in the SmA-Hex$B$ transition. This is the case of strong coupling between smectic order (θ) and hexatic order (φ), and has been observed recently [14]. On the other hand, when the coupling between smectic order (θ) and hexatic order (φ) vanishes, the Hex$B$-SmA transition displays a very weak singularity and is consistent with the KT transition [15]. It is observed in Figs. 2(a) and 3(a) that the curves marked (a) for $B=0$ and (b) for $B<0.3$ correspond to the KT transition with its characteristic hump of the heat capacity. The curves (c) and (d) for $B>0.4$ imply the strong coupling between hexatic and smectic order, which results in the Hex$B$-SmA transition with strong singularity and displays the characteristic phase transition of weak first order. As a result of the strong coupling between hexatic and smectic order, Θ_n displays a distinct drop when Φ_n jumps to zero as is seen in Figs. 2(b), 3(b), and 4, which results in a Hex$B$-SmA transition with strong singularity.

Finally, let us take a look at a different arrangement of molecules in the structure shown in Fig. 1(b). The molecule at (0, 0, 0) has eight nearest neighbors at $(a,0,0)$, $(-a,0,0)$,

$$\left(-\frac{1}{2}a,\frac{\sqrt{3}}{2}a,0\right),\left(\frac{1}{2}a,-\frac{\sqrt{3}}{2}a,0\right),$$

$$\left(-\frac{1}{2}a,-\frac{\sqrt{3}}{2}a,0\right),\left(\frac{1}{2}a,\frac{\sqrt{3}}{2}a,0\right)$$

in the same layer, and $(0,0,\pm c)$ in adjacent layers. There are twelve second nearest neighbors at $(a,0,\pm c)$, $(-a,0,\pm c)$,

$$\left(-\frac{1}{2}a,\frac{\sqrt{3}}{2}a,\pm c\right),\left(\frac{1}{2}a,-\frac{\sqrt{3}}{2}a,\pm c\right),$$

$$\left(-\frac{1}{2}a,-\frac{\sqrt{3}}{2}a,\pm c\right),\left(\frac{1}{2}a,\frac{\sqrt{3}}{2}a,\pm c\right)$$

in the adjacent layers. The interlayer interaction for hexatic order between (0, 0, 0) and its nearest neighbors in the adjacent layer is zero, while that between (0, 0, 0) and its second nearest neighbors is larger than zero, namely, $Q'>0$. However, we have seen that the multiple heat capacity anomaly would vanish once $Q'/Q \geqslant 0.1\%$. As an example, only two of the original three heat-capacity peaks of a six-layer film can be found in Fig. 7 when $Q'/Q=1/411$, indicating that the direct interlayer interaction for hexatic order would baffle the observed multiple heat-capacity anomaly. Hence, this molecular arrangement is not appropriate for our model, while our model of a close-packed structure is reasonable, as its direct interlayer interaction is very small and results in hexatic disorder.

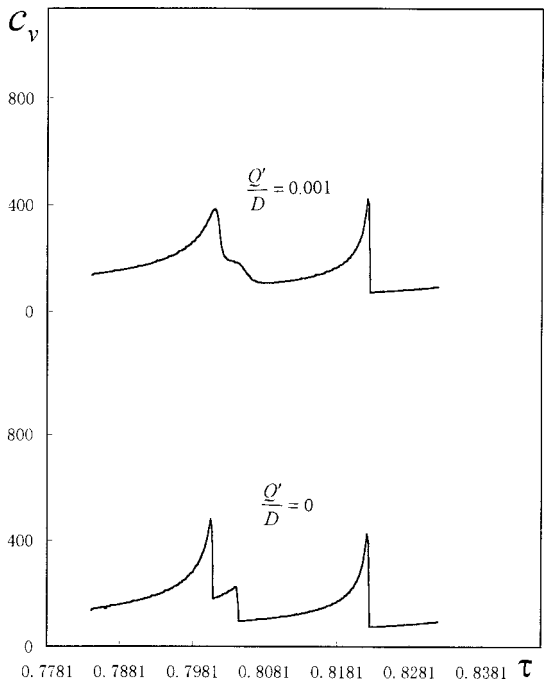

FIG. 7. The reduced heat capacity c_v of a six-layer film versus reduced temperature τ. (a) $Q'/D=0$ and (b) $Q'/D=0.001$.

Recent experiments [14,16,17] for a two-layer 54COOBC film observed other phases (the so-called HexB_1 and HexB_2 or SmA' and Hex$B$) in a hexatic liquid crystal. Therefore, in the forthcoming paper we would expand our unified model and introduce an order parameter $\langle\cos(6\varphi)\rangle$ [18] by applying the same microscopic method we developed in this paper.

ACKNOWLEDGMENT

Two of us (L. P. Shi and J. Shi) are grateful to the Natural Science Foundation of China for financial support under Grant No. 19474073.

[1] W. Maier and A. Saupe, Z. Naturforsch Z. Naturforsch. A **13A**, 564 (1958); **14A**, 882 (1959); **15A**, 287 (1960).
[2] W. J. A. Goosens, Mol. Cryst. Liq. Cryst. **12**, 237 (1971).
[3] W. L. Mcmillan, Phys. Rev. A **4**, 1238 (1971); **6**, 936 (1972).
[4] B. I. Halperin and D. R. Nelson, Phys. Rev. Lett. **41**, 121 (1978); R. Bruinsma and D. R. Nelson, Phys. Rev. B **23**, 402 (1981); D. R. Nelson and B. I. Halperin, *ibid.* **21**, 5312 (1980); **19**, 2457 (1979).
[5] V. M. Kaganer and M. A. Osipov, J. Chem. Phys. **109**, 2600 (1998).
[6] J. Shi and L. P. Shi, Phys. Lett. A **245**, 256 (1998).
[7] T. Stoebe, P. Mach and C. C. Huang, Phys. Rev. Lett. **73**, 1384 (1994).
[8] A. J. Jin, Ph.D. dissertation, University of Minnesota, 1996, Chap. 4.
[9] R. Pindak, D. E. Moncton, S. C. Davey, and J. W. Goodby, Phys. Rev. Lett. **46**, 1135 (1981); R. J. Birgeuean and J. D. Litster, J. Phys. (France) Lett. **39**, 399 (1978).
[10] J. D. Brook, A. Aharony, R. J. Birgeuean, K. W. Evaus-Luttesodt, J. D. Litster, P. M. Horn, B. Stephenson and A. R. Tajbakhsh, Phys. Rev. Lett. **57**, 98 (1986).
[11] E. B. Sirota, P. S. Pershan, S. Amador, and L. B. Sorensen,

Phys. Rev. A **35**, 2283 (1987).
[12] S. Amador, P. S. Pershan, H. Stragier, B. D. Swanson, D. J. Twest, L. B. Sorensen, E. B. Sirota, G. E. Ice, and A. Habenschiss, Phys. Rev. A **39**, 2703 (1989).
[13] A. J. Jin, M. Veum, T. Stoebe, C. F. Chou, J. T. Ho, S. W. Hui, V. Surendranath, and C. C. Huang, Phys. Rev. Lett. **74**, 4863 (1995).
[14] C. Y. Chao, S. W. Hui, J. E. Maclennan, C. F. Chou, and J. T. Ho, Phys. Rev. Lett. **78**, 2581 (1997).
[15] J. M. Kosterlitz and D. J. Thouless, J. Phys. C **6**, 1181 (1973).
[16] C. F. Chao, J. T. Ho, S. W. Hui, and V. Surendranath, Phys. Rev. Lett. **76**, 4556 (1996).
[17] C. F. Chou, J. T. Ho, and S. W. Hui, Phys. Rev. E **56**, 592 (1997).
[18] L. P. Shi and J. Shi (unpublished).